Journal of Physics: Conference Series **640** (2015) 012022 doi:10.1088/1742-6596/640/1/012022

First-principles calculation of the structural and elastic properties of ternary metal nitrides $Ta_xMo_{1-x}N$ and $Ta_xW_{1-x}N$

Kh. Bouamama[1]*, P. Djemia[2] and M. Benhamida[1]
[1]LOC, Département de Physique, Université Ferhat Abbas, 19000 Sétif, Algeria.
[2]LSPM-CNRS, Sorbonne Paris Cité, Université Paris 13, 99 Avenue J.B. Clément, 93430 Villetaneuse, France.

E-mail: khaled_bouamama@univ-setif.dz

Abstract: First-principles pseudo-potentials calculations of the mixing enthalpy, of the lattice constants a_0 and of the single-crystal elastic constants c_{ij} for ternary metal nitrides $Ta_xMe_{1-x}N$ (Me=Mo or W) alloys considering the cubic B1-rocksalt structure is carried out. For disordered ternary alloys, we employ the virtual crystal approximation VCA in which the alloy pseudo-potentials are constructed within a first-principles VCA scheme. The supercell method SC is also used for ordered structures in order to evaluate clustering effects. We find that the mixing enthalpy still remains negative for $Ta_xMe_{1-x}N$ alloys in the whole composition range which implies these cubic $Ta_xMo_{1-x}N$ and $Ta_xW_{1-x}N$ ordered solid solutions are stable. We investigate the effect of Mo and W alloying on the trend of the mechanical properties of TaN. The effective shear elastic constant c_{44}, the Cauchy pressure (c_{12}-c_{44}), and the shear to bulk modulus G/*B* ratio are used to discuss, respectively, the mechanical stability of the ternary structure and the brittle/ductile behavior in reference to TaN, MeN alloys. We determine the onset transition from the unstable structure to the stable one B1-rocksalt from the elastic stability criteria when alloying MeN with Ta. In a second stage, in the frame of anisotropic elasticity, we estimate by one homogenization method the averaged constants $<C_{ij}>$ of the polycrystalline $Ta_xMe_{1-x}N$ alloys considering the special case of an isotropic medium with no crystallographic texture.

1. Introduction

Materials that combine both hardness and ductility are said tough materials, with a high resistance to failure [1]. In bulk materials, toughness is easily extracted from uniaxial compression or tensile tests by measuring the area under the curve of the stress-strain curve, whereas for coatings it is not well established. The design and development of such materials have always been a challenge, because an increase in hardness is usually accompanied by an increase in brittleness rather than ductility. One of the major goals of materials scientists and hard coating industries has been the development of hard materials (bulk, coatings or multilayers) with high temperature stability [2-6]. While high hardness is indispensable, most applications also demand ductility in order to avoid brittle failure due to cracking in coatings exposed to high stresses. However, hard refractory ceramics such as transition metal TM based nitrides are in general brittle. Enhancement of toughness can be obtained by the inhibition of both crack initiation and propagation. In case of polycrystalline materials, grain boundaries are the structurally weaker regions where the cracks will spread along. Since the crack size is generally proportional to the grain size, the propensity for crack propagation can also be attenuated by decreasing the size of grains or flaws to the nanoscale [7]. Such nanostructuring can be obtained by

developing hard and tough ceramic coatings via the synthesis of nanoscale composites [7-9] achieved via many routes [7, 10-15]. Fundamental understanding of the origins of toughness is not widely studied, while progress in this area can only be achieved through atomic- and electronic-level understanding of the origins of brittleness *vs*. ductility. Such studies are, however, relatively few [16-19]. *Ab initio* theoretical studies, using density functional theory DFT calculations, are well adapted for such design by providing information concerning the relationship between electronic structure and mechanical properties. This work aims to benefit from existing DFT studies of toughness enhancement to predict tough TM nitrides that could be later deposited as coatings. In this paper, we investigate the stability, the structural and the elastic properties of $Ta_xMe_{1-x}N$ (Me = Mo and W) alloys by DFT calculations on both disordered ordered alloys. The evolutions of the lattice parameters a_0, of the density of electronic states DOS and of the single-crystal elastic constants c_{ij} as a function of x, are determined. The effective elastic constants and moduli of isotropic polycrystalline materials are computed using a Voigt-Reuss-Hill [20] model. Predictive ductility behavior of the polycrystalline alloys is discussed in terms of Pettifor [21] and Pugh criteria [22] in relation to their elastic properties.

2. The computational method

The calculations are performed with the density-functional perturbation theory DFPT in the plane-wave pseudo-potential method as implemented in the ABINIT code [23]. This is done with the self-consistent response function computations for electric field perturbations and the ionic displacements [24-27]. For the exchange-correlation potential, we used the generalized gradient approximation (GGA) of Perdew, Burke and Ernzerhof (PBE) [28, 29]. The atoms are represented by norm-conserving optimized [30] designed nonlocal [31] pseudo-potentials, generated with the OPIUM code [32], where the semi-core p states were included because of their importance for good transferability. The Brillouin zone integrations were replaced by discrete summations over a special set of k-points using the standard technique of Monkhorst and Pack [33], where the k-points mesh used is (16 x 16 x 16) and the plane-wave energy cutoff to expand the wave functions is set to be 80 Hartree (1 Ha = 27.2116 eV) to get a total energy accuracy better than 10^{-5} Hartree. The Fermi-Dirac smearing approach [34, 35] is used with a cold smearing of 0.005 Hartree. For the treatment of the disordered ternary alloy, we have used the virtual crystal approximation VCA implemented in the ABINIT program, in which the alloy pseudo-potentials are constructed within a first-principles VCA scheme. Elemental ionic pseudo-potentials of MeN (Me = Mo or W) and TaN are combined to construct the virtual pseudo-potential of the $Ta_xMe_{1-x}N$, *i.e.*:

$$V_{VCA} = xV_{TaN} + (1-x)V_{MeN} \quad (1)$$

Simple cubic 8-atoms supercells, containing 1 (x=0.25), 2 (x=0.5) and 3 (x=0.75) substitutional Ta atoms on the Me sites were used to describe the $Ta_xMe_{1-x}N$ ordered compounds.

3. Results and discussion

3.1. Phase stability, structural and electronic properties analysis

The mixing energy enthalpy equivalent to the Gibbs free energy at T=0 K, is defined as:

$$\Delta E_{Ta_xMe_{1-x}N}(x) = E_{Ta_xMe_{1-x}N} - (1-x)E_{MeN} - xE_{TaN} \quad (2)$$

with $E_{Ta_xMe_{1-x}N}$ the total energy per atom of the $Ta_xMe_{1-x}N$ alloy, E_{MeN} and E_{TaN} the total energy per atom of MeN and TaN alloys, respectively. The calculated mixing energies ΔE of $Ta_xMe_{1-x}N$ alloys with rocksalt structure using SC are shown is Fig. 1. They are negative, indicating that MeN and TaN may continuously form stable solid solutions in comparison to the phase-separated MeN+TaN. The mixing energy of $Ta_xMo_{1-x}N$ is much lower than that of $Ta_xW_{1-x}N$, indicative of a better thermal stability of $Ta_xMo_{1-x}N$ over $Ta_xW_{1-x}N$.

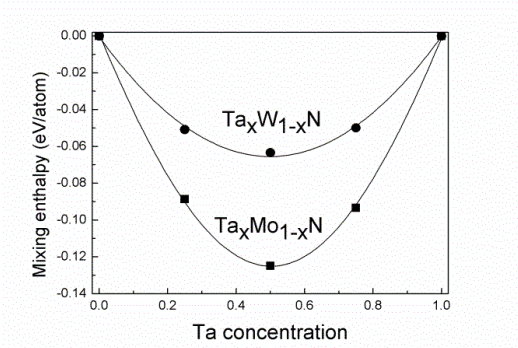

Figure 1. SC computed mixing enthalpy of $Ta_xMe_{1-x}N$ alloys as a function of Ta concentration, x.

DOS of $Ta_xMe_{1-x}N$ is presented in Fig. 2. The main features of DOSs of $Ta_xMo_{1-x}N$ and $Ta_xW_{1-x}N$ are very similar to each other. The energy region from −10 to −4 eV is characterized by the strong hybridization of the Me-d electrons of the metals with the N-p electrons, which is at the origin of the covalent-like bonding in these materials resulting to high strength and high hardness. The energy region from−4 to 7 eV shows energy states filled mainly by the Ta-d and Me-d electrons and a small contribution of the N-p electrons. These strong metal-metal bonds should contribute to a better ductility as the metallic states become more populated with the introduction of Mo or W. Such materials offer the combination of strong covalent bonds Me-N with metallic bonds Me-Ta conferring both strength and ductility, and then toughness.

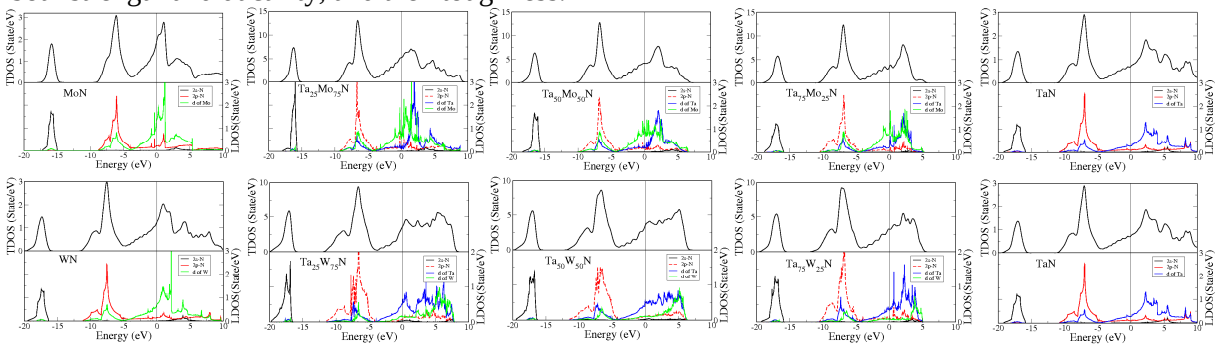

Figure 2. Total electronic density of states (TDOS) and local electronic density of states (LDOS) for the $Ta_xMe_{1-x}N$ alloys calculated with ABINIT-SC. Zero energy stands for the Fermi level and is denoted by vertical black lines.

The lattice parameters a_0 of $Ta_xMe_{1-x}N$ are shown in Fig. 3, for both VCA and SC methods, as a function of TaN composition, *x*. For $Ta_xMo_{1-x}N$, a_0 decreases from 0.4384 nm for MoN to 0.4316 nm for TaN with increasing *x*. However, for $Ta_xW_{1-x}N$, a_0 remains constant. The relative difference between VCA and SC calculations does not exceed 0.3% with a negative bowing from the Vegard's rule for VCA. We find a good agreement between our calculated lattice parameters for binary alloys WN, MoN and TaN and the calculated lattice parameters, WN (0.435 nm) [36], MoN (0.433 nm) [37] and the experimental δ-TaN (0.4336 nm) [38, 39].

3.2. Elastic properties

The single crystal elastic constants c_{ij} of $Ta_xMe_{1-x}N$ are shown in Fig. 4 for both VCA and SC methods with the bulk modulus $B = (c_{11}+2c_{12})/3$. For both alloys, the c_{11} and c_{44} elastic constants increase as a function of x, while the c_{12} decreases. B remains constant for $Ta_xW_{1-x}N$ alloys (375±3 GPa) and for $Ta_xMo_{1-x}N$ alloys *B* slightly increases from MoN (306 GPa) to TaN (373 GPa). The obtained values for the elastic constants and B for TaN are in good agreements with the calculated ones [40].

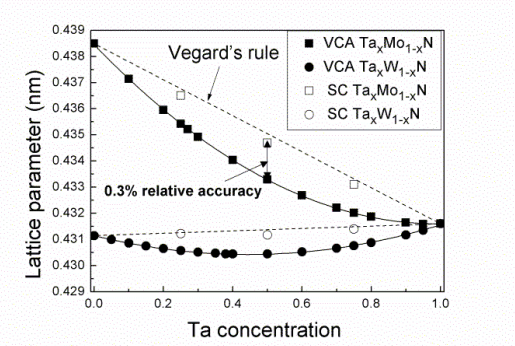

Figure 3. VCA calculated (plain symbols) and SC calculated (empty symbols) lattice parameters of $Ta_xMe_{1-x}N$ as a function of x. Dotted lines are the Vegard's rule from the binary alloys TaN and MeN.

The Born elastic stability criteria (B>0, c_{11}-c_{12}>0, c_{44}>0) are satisfied for $Ta_xMo_{1-x}N$ alloys with x>0.27 and for $Ta_xW_{1-x}N$ alloys with x>0.38 (see fig. 4). Adding Ta to MoN or WN enables to stabilize the B1-rocksalt structure above these critical amount of Ta $(x_{Ta})_{cr,MeN}$.
Using the calculated single-crystal stiffnesses c_{ij}, we performed a Voigt-Reuss-Hill average leading to the effective constants $<C_{11}>$, $<C_{12}>$ and $<C_{44}>$ of polycrystalline $Ta_xMo_{1-x}N$ and $Ta_xW_{1-x}N$ considering a random orientation of crystallites [20]. Afterwards, the Young modulus E and the Poisson ratio σ of the polycrystals are calculated from the Eq. (3-4) for isotropic elastic symmetry:

$$E = C_{11} - 2\,C_{12}^2/(C_{11} + C_{12}) \quad (3)$$
$$\sigma = C_{12}/(C_{11} + C_{12}) \quad (4)$$

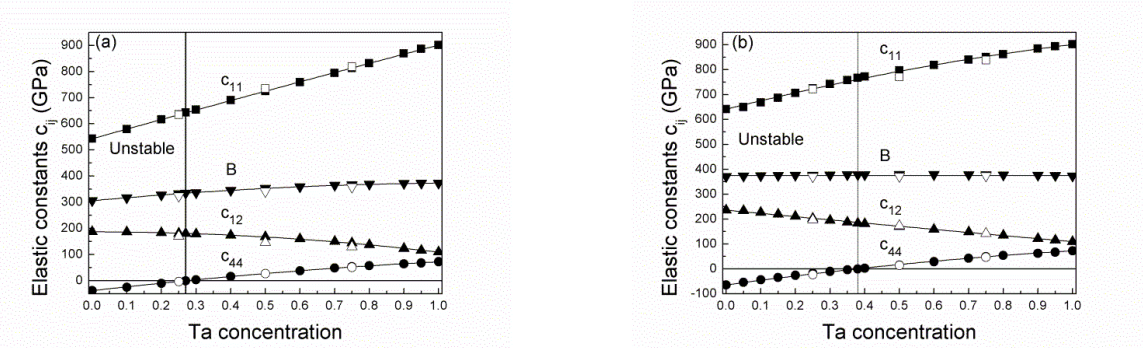

Figure 4. VCA calculated (plain symbols) and SC calculated (empty symbols) elastic constants c_{ij} and the bulk modulus B for (a) $Ta_xMo_{1-x}N$ and (b) $Ta_xW_{1-x}N$ as a function of Ta concentration, x. The vertical line indicates the transition from mechanically unstable → stable.

The shear modulus G is simply $<C_{44}>$. The $<C_{ij}>$ are plotted in Fig. 5 for both VCA and SC methods and the elastic moduli in Fig. 6. For both alloys, effective elastic constants remain close from each other. The $<C_{11}>$ and $<C_{44}>$ elastic constants increase as a function of x, while the $<C_{12}>$ decreases.
In Fig. 6, E increases from $Ta_{0.3}Mo_{0.7}N$ (138 GPa) and from $Ta_{0.4}W_{0.6}N$ (50 GPa) to TaN (353 GPa). However, σ decreases from $Ta_{0.3}Mo_{0.7}N$ (0.432) and from $Ta_{0.4}W_{0.6}N$ (0.477) to TaN (0.333).
Pettifor [21] proposed that Cauchy pressure, defined as $p = c_{12}$-c_{44}, can be used as an indicator to classify a material as brittle or ductile. The changes in p are connected with the nature of the atomic bonding. If the bonding is more metallic, $p > 0$, while for more brittle materials with directional bonding, $p < 0$.

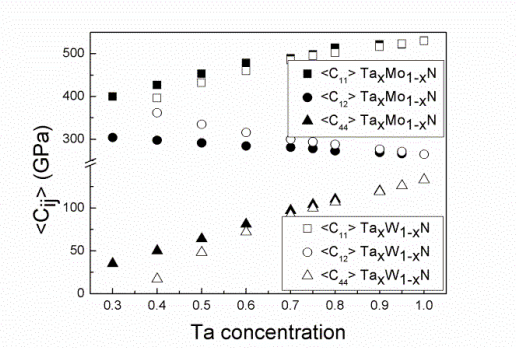

Figure 5. VCA calculated effective elastic constants $<C_{11}>$, $<C_{12}>$, $<C_{44}>$ of $Ta_xMo_{1-x}N$ (plain symbols) and $Ta_xW_{1-x}N$ (empty symbols) alloys as a function of Ta concentration, x.

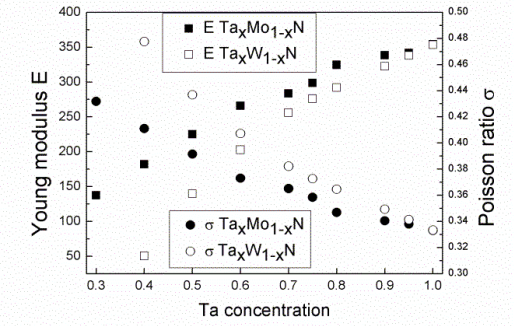

Figure 6. Effective elastic moduli (E, σ) considering non crystallographic texture for cubic polycrystalline $Ta_xMo_{1-x}N$ (plain symbols) and $Ta_xW_{1-x}N$ (empty symbols) alloys as a function of x.

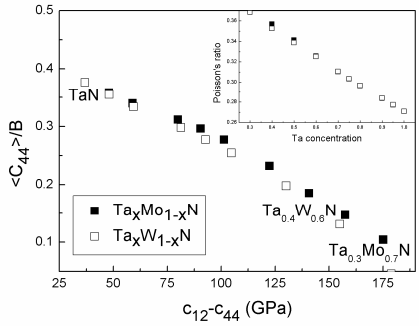

Figure 7. Map of brittleness and ductility of $Ta_xMe_{1-x}N$ disordered polycrystalline alloys.

The Fig. 7 shows that polycrystalline $Ta_xMe_{1-x}N$ have a ductile behavior, considering both the Pettifor criterion ($p > 0$) for ductile materials and the Pugh criterion [22] (G/B <0.5). One can also notice that $\sigma > 0.25$. p increases while G/B reduces with addition of Mo or W increasing ductility.

4. Summary and conclusion

The lattice constants, the mixing enthalpy, the bulk modulus, the single-crystalline elastic constants of the ternary nitrides alloys $Ta_xMe_{1-x}N$ (Me= Mo or W) are calculated as a function of x, using a first-principles pseudo-potential approach within the VCA for disordered alloys and the SC method for ordered alloys using GGA exchange-correlation potential. A negative bowing is observed for the lattice constants in comparison to the Vegard's rule for VCA calculations. SC mixing enthalpies are negative and indicate that both alloys are energetically stable in reference to their binary counterparts. We obtain close results for the elastic constants between VCA and SC calculations indicating a little

influence of the ordering/clustering of metal atoms. c_{44} is positive above a critical Ta concentration $(x)_{cr,MoN}$~0.27 < $(x)_{cr,WN}$~0.38 above which the B1-rocksalt structure is mechanically stable. From Pettifor (c_{12}-c_{44}>0) and Pugh (G/B<0.5) criteria the ductility of the alloys are found to increase as more Mo or W is added. Close effective elastic properties of both alloys are observed above x~0.7.

5. References

[1] Dieter GE and Bacon DJ: *Mechanical Metallurgy* 1988 MCGRAW-HILL Higher Education.
[2] Hugosson HW, Jansson U, Johansson B and Eriksson O 2001 *Science* **293** 2434.
[3] Joelsson T, Hultman L, Hugosson HW and Molina-Aldareguia JM 2005 *Appl. Phys. Lett.* **86** 131922.
[4] Helmersson U, Todorova S, Barnett S, Sundgren JE, Markert LC and Greene J 1987 *J. Appl. Phys.* **62** 481.
[5] Veprek S, Veprek-Heijman MGJ, Karvankova P and Prochazka J 2005 *Thin Solid Films* **476** 1.
[6] Shin CS, Gall D, Hellgren N, Patscheider J, Petrov I and Greene JE 2003 *J. Appl. Phys.* **93** 6025.
[7] Zhang S, Sun D, Fu Y and Du H 2005 *Surf. Coat. Tech.* **198** 2.
[8] Zhang S, Wang HL, Ong SE, Sun D and Bui XL 2007 *Plasma Processes and Polymers* **4** 219.
[9] Abadias G, Ivashchenko VI, Belliard L and Djemia P 2012 *Acta Materiala* **60** 5601.
[10] Djemia P, Benhamida M, Bouamama Kh, Belliard L, Faurie D and Abadias G 2013 *Surf. Coat. Tech.* **215** 199.
[11] Anton D and Shah D 1990 In *MRS Proceedings*: Cambridge Univ Press: **194** 45.
[12] Abe O and Ohwa Y 2004 *Solid State Ionics* **172** 553.
[13] Zhan GD, Kuntz JD, Wan JL and Mukherjee AK 2003 *Nature Materials* **2** 38.
[14] Basu B, Venkateswaran T and Kim DY 2006 *Journal of the American Ceramic Society* **89** 2405.
[15] Zhang S, Sun D, Fu Y and Du H 2003 *Surf. Coat. Tech.* **167** 113.
[16] Hogmark S, Jacobson S and Larsson M 2000 *Wear* **246** 20.
[17] Kamran S, Chen KY and Chen L 2009 *Phys. Rev. B.* **79** 024106.
[18] Dasgupta T, Waghmare UV and Umarji AM 2007 *Phys. Rev. B.* **76** 174110.
[19] Abadias G, Kanoun MB, Goumri-Said S, Koutsokeras L, Dub SN and Djemia Ph 2014 *Phys. Rev. B.* **90** 144107.
[20] Hill R 1952 *Proc. Phys. Soc.* A **65** 349.
[21] Pettifor DG 1992 *Mater. Sci. Technol.* **8** 345.
[22] Pugh SF 1954 *Philos. Mag.* **45** 823.
[23] Gonze X *et al*. 2009 *Computer Physics Communications* **180** 2582.
[24] Giannozzi P, de Gironcoli S, Pavone P and Baroni S 1991 *Phys. Rev. B.* **43** 7231.
[25] Gonze X 1997 *Phys. Rev. B.* **55** 10337.
[26] Gonze X and Lee C 1997 *Phys. Rev. B.* **55** 10355.
[27] Ghosez Ph, Michenaud JP and Gonze X 1998 *Phys. Rev. B.* **58** 6224.
[28] Perdew JP, Burke K and Ernzerhof M 1996 *Phys. Rev. Lett.* **77** 3865.
[29] Perdew JP and A. Zunger 1981 *Phys. Rev. B.* **23** 5048.
[30] Rappe AM, Rabe KM, Kaxiras E and Joannopoulos JD 1990 *Phys. Rev. B.* **41** 1227.
[31] Ramer NJ and Rappe AM 1999 *Phys. Rev. B.* **59** (1999) 12471.
[32] http://opium.sourceforge.net
[33] Monkhorst HJ and Pack JD 1976 *Phys. Rev. B.* **13** 5189.
[34] Fu CL and Ho KM 1983 *Phys. Rev. B.* **28** 5480.
[35] Methfessel M and Paxton AT 1989 *Phys. Rev. B.* **40** 3616.
[36] Isaev EI *et al.* 2007 *J. Appl. Phys.* **101** 123519.
[37] Chen W and Jiang JZ 2010 *Journal of alloys and compounds* **499** 243.
[38] Mashimo T, Tashiro S, Nishida M, Miyahara K and Eto E 1997 *Physica* B **239** 13.
[39] Abadias G, Belliard L and Djemia P 2014 *Surf. Coat. Tech.* **257** 129.
[40] Zhao E and Wu Z 2008 *Journal of Solid State Chemistry* **181** 2814.